

# Super-Universality in Anderson Localization

Ivan Horváth<sup>1,2,\*</sup> and Peter Markoš<sup>3,†</sup>

<sup>1</sup>University of Kentucky, Lexington, KY 40506, USA

<sup>2</sup>Nuclear Physics Institute CAS, 25068 Řež (Prague), Czech Republic

<sup>3</sup>Dept. of Experimental Physics, Faculty of Mathematics, Physics and Informatics, Comenius University in Bratislava, Mlynská Dolina 2, 842 28 Bratislava, Slovakia

(Dated: Oct 21, 2021)

We calculate the effective spatial dimension  $d_{\text{IR}}$  of electron modes at critical points of 3D Anderson models in various universality classes (O,U,S,AIII). The results are equal within errors, and suggest the super-universal value  $d_{\text{IR}} = 2.665(3) \approx 8/3$ . The existence of such a unique marker may help identify natural processes driven by Anderson localization, and provide new insight into the spatial geometry of Anderson transitions. The recently introduced  $d_{\text{IR}}$  is a measure-based dimension of Minkowski/Hausdorff type, designed to characterize probability-induced effective subsets.

Keywords: Anderson localization, effective dimension, universality, symmetry, effective number, measure

**1. Introduction.** Localization of quantum particles [1] is an important effect influencing the transport properties of mesoscopic systems. Following a 1-parameter scaling theory [2], the transition from extended (metallic) to localized (insulating) state takes place at a critical point. In a prototypical Anderson model realization, this occurs on a critical line in  $(E, W)$  plane, where  $E$  is the Fermi energy and  $W$  the strength of a random potential. After years of theoretical and numerical investigation (see e.g. [3]) it is generally accepted that these Anderson transitions are universal. There are ten universality classes [4] with distinct values of critical exponents  $\nu$  and  $s$  describing the approach to criticality from the localized and extended sides respectively. Given that these indices are coupled [5], many numerical works evaluated  $\nu$  and the value  $W_c$  of disorder at the canonical critical point  $(0, W_c)$ , especially for the 3D orthogonal class (see e.g. [6–8]).

Among key attributes of a transition to localized state is that it drastically reduces the volume effectively accessible by a particle. Here we describe this effect in a meaningful quantitative manner. Note that it is not the endpoint of the Anderson transition that is interesting in this regard. Indeed, the known feature of exponentially bounded wave function (exponential localization) provides the relevant information in that case. Rather, it is the intermediate step toward localization, the critical state, that is of primary interest here. Indeed, we will describe Anderson criticality in terms of particle’s propensity to occupy the volume of space nominally available to it.

At the heart of such description is the notion of effective volume. Since ordinary volume is an important physical attribute of a system, so is its effective counterpart if it can be put on a similar conceptual footing. In other words, if it can be interpreted as a geometric characteristic expressing the amount of occupied space (its measure), and is not too arbitrary so as to be uninformative. Such issues have recently been successfully resolved [9–11]. Here we will use these results, reviewed in Sec.2, to work with properly defined effective volumes of Anderson eigenmodes.

A robust characteristic of a critical point needs to involve thermodynamic ( $L \rightarrow \infty$ ) limit in order to capture its non-analyticity. Thus, consider Anderson lattice system in  $D$  dimensions so that its volume  $V(L) \propto L^D$ . The effective volume  $V_{\text{eff}}(L, E) \leq V(L)$  occupied by electron at energy  $E$  may scale differently, namely  $V_{\text{eff}}(L, E) \propto L^{d_{\text{IR}}(E)}$ , for  $L \rightarrow \infty$ , where  $d_{\text{IR}}(E) \leq D$ . The *effective dimension*  $d_{\text{IR}}$ , first used in the context of QCD Dirac eigenmodes [11], properly quantifies the property we seek. Note that, if  $d_{\text{IR}} < D$ , the particle occupies space of measure zero relative to nominal space in  $L \rightarrow \infty$  limit ( $V_{\text{eff}}/V \rightarrow 0$ ). The value  $D - d_{\text{IR}}$  gives the rate at which modes lose the ability to fill the growing space.

Since  $d_{\text{IR}}$  is a strictly infrared (IR) quantity [11], it is a natural characteristic of criticality that transforms spatial features. In that vein,  $d_{\text{IR}}$  is expected to be universal in Anderson transitions, even though it doesn’t enter the standard scaling theory [2]. However, in this Letter we present evidence for something unexpected, namely that  $d_{\text{IR}}$  is in fact *super-universal*: it expresses commonality existing across the symmetry classes. More concretely, we find that  $d_{\text{IR}} \approx 8/3$  for classes O, U, S and AIII, with errors (couple parts per mill) comparable to their mutual differences. The stark difference between the usual universality (via  $\nu$ ) and the proposed super-universality (via  $d_{\text{IR}}$ ) can be seen from the comparison shown in Table I.

**2. Effective Volume and IR Dimension.** Volume  $V = a^D N$  of a hypercubic system with lattice constant  $a$  can be thought of as determined by counting the lattice sites ( $N$ ). Its measure-like nature then stems from additivity of ordinary counting: the total is the sum of counts for parts. Similarly, the effective volume  $V_{\text{eff}}[\psi] = a^D \mathcal{N}[\psi]$  occupied by wave function  $\psi$  is determined by effective counting ( $\mathcal{N}$ ) which takes into account that  $\psi$  endows lattice sites with probabilities, and hence varied relevance. For  $V_{\text{eff}}$  to be measure-like, the underlying effective counting also has to be additive.

The effective number theory of Ref. [9] determines all consistent additive schemes to count collections of objects

arXiv:2110.11266v1 [cond-mat.dis-nn] 21 Oct 2021

$(o_1, o_2, \dots, o_N)$  with probabilities  $P = (p_1, p_2, \dots, p_N)$ . Each scheme is represented by function  $\mathcal{N} = \mathcal{N}[P]$  on discrete probability distributions. A key result is the existence of a scheme  $\mathcal{N}_\star$  satisfying  $\mathcal{N}_\star[P] \leq \mathcal{N}[P]$  for all  $P$  and  $\mathcal{N}$ . This minimal effective amount, specified by

$$\mathcal{N}_\star[P] = \sum_{i=1}^N \mathbf{n}_\star(Np_i) \quad , \quad \mathbf{n}_\star(c) = \min\{c, 1\} \quad (1)$$

is inherent to each collection<sup>1</sup>, and has absolute meaning.

Effective dimension  $d_{\text{IR}}$  is based on  $\mathcal{N}_\star$  [9, 11, 12]. The explicit definition for Anderson systems starts with eigenfunction  $\psi = \psi(x_i, E, W, L, \zeta)$  at a particular realization  $\zeta$  of microscopic disorder with strength  $W$ . The associated probabilities are  $p_i = \psi^\dagger \psi(x_i)$ , and  $d_{\text{IR}}(E, W)$  arises via

$$\langle \mathcal{N}_\star \rangle_{E, W, L} \propto L^{d_{\text{IR}}(E, W)} \quad \text{for } L \rightarrow \infty \quad (2)$$

where  $\langle \dots \rangle$  is the disorder average involving states from the spectral vicinity of  $E$ . Here we will be interested in  $d_{\text{IR}}(0, W_c)$  for models from O, U, S and AIII symmetry classes. Their critical values  $W_c$ , listed in Table I, are known to high accuracy.

**3. Anderson Models.** All models we study are defined on  $L^3$  cubic lattice with each site  $r = (x, y, z)$  supporting two quantum states. Disorder is introduced via random energies  $\epsilon_r$  chosen from a box distribution in the range  $[-W/2, +W/2]$ . Hopping terms in the Hamiltonian only connect the nearest neighbors. They are described by  $2 \times 2$  matrices  $t_{r, e_j}$ , one for each  $r$  and direction specified by the unit lattice vector  $e_j$  ( $j = x, y, z$ ). The Hamiltonian is

$$\mathcal{H} = \sum_r \epsilon_r c_r^\dagger \sigma_{\text{diag}} c_r + \sum_{r, j} c_r^\dagger t_{r, e_j} c_{r-e_j} + h.c. \quad (3)$$

where operators  $c_r$  have two components and  $\sigma_{\text{diag}}$  is diagonal. In definitions of specific models below,  $\sigma_0$  denotes the identity matrix and  $\sigma_j$  the Pauli matrices. Periodic boundary conditions are imposed in all cases.

**Orthogonal (O):**  $\sigma_{\text{diag}} = t_{r, e_j} = \sigma_0$ .

model	Ref	$W_c$	$\nu$	$d_{\text{IR}}(\text{here})$
O	[8]	16.543(2)	1.572(5)	2.664(2)
U	[7]	18.375(17)	1.43(6)	2.665(3)
S	[13]	19.099(9)	1.360(6)	2.662(4)
A	[14]	11.223(20)	1.071(4)	2.668(4)

TABLE I. Critical parameters of 3D orthogonal (O), unitary (U), symplectic (S) and AIII (A) symmetry classes. Their meaning is discussed in the text.

<sup>1</sup> It is inherent because it cannot be reduced by redefinition of a counting scheme. When applied to uncertainty in quantum mechanics, this leads to the notion of intrinsic uncertainty [10].

**Unitary (U):**  $\sigma_{\text{diag}} = t_{r, e_x} = t_{r, e_y} = \sigma_0$  and  $\theta = 1/4$  [15] in

$$t_{r, e_z} = \sigma_0 \exp(-i2\pi\theta x) \quad (4)$$

**Symplectic Ando (S):**  $\sigma_{\text{diag}} = \sigma_0$  and  $\theta = \pi/6$  [13] in

$$t_{r, e_j} = \exp(i\theta\sigma_j) \quad (5)$$

**AIII (A):**  $\sigma_{\text{diag}} = \sigma_z$ . We use  $t_{\parallel} = 0.4$  in  $t_{r, e_z} = t_{\parallel}\sigma_0$ , and  $t_{\perp} = 0.5$ ,  $t_{\perp} = 0.6$  [14] in

$$t_{r, e_x} = t_{\perp}\sigma_0 + it_{\perp}\sigma_x \quad , \quad t_{r, e_y} = t_{\perp}\sigma_0 + it_{\perp}\sigma_y \quad (6)$$

We note that in O, U and S models, all energy eigenvalues are doubly degenerate, while in the chiral A model they come in  $(-E, E)$  pairs for each sample of disorder.

**4. Technical Details.** We use JADAMILU library [16] to numerically diagonalize 1-particle Anderson Hamiltonians. For each sample of disorder, we compute 10 distinct eigenvalues closest to  $E=0$  and all associated eigenstates. This results in probing a very small vicinity of the band center for all studied systems, e.g.  $|E| \lesssim 5 \cdot 10^{-3}$  for O at  $L = 24$  with  $L^{-3}$  size dependence. Hence, all computed states are included in the estimate (simple average) of  $\mathcal{N}_\star$  associated with a given sample. Disorder average is then performed by accumulating  $5-20 \times 10^3$  independent samples. The sizes of studied systems range from  $L = 8$  to  $L = 128$  (O), 112 (U), and 72 (S) and (A).

As an intermediate step toward extracting the dimension  $d_{\text{IR}}$ , we define its finite- $L$  counterpart from ratios of effective volumes on systems with sizes  $L$  and  $L/s$

$$d_{\text{IR}}(L, s) \equiv \frac{1}{\ln s} \ln \frac{\langle \mathcal{N}_\star \rangle_L}{\langle \mathcal{N}_\star \rangle_{L/s}} \quad , \quad s > 1 \quad (7)$$

Given the defining asymptotic behavior (2), we can then use that  $d_{\text{IR}} = \lim_{L \rightarrow \infty} d_{\text{IR}}(L, s)$ , independently of  $s$ . The latter can be adjusted to suit the available range of sizes and statistics. We will use  $s=2$  which is also convenient due to a large number of pairs  $(L, L/2)$  accessible by the lattice geometry. Note that, since the data at different  $L$  are independent, the error  $\Delta$  of  $d_{\text{IR}}(L, s)$  can be estimated via simple error propagation from errors  $\delta$  of  $\mathcal{N}_\star$ . In particular,  $\Delta(L, s) = \sqrt{\delta^2(L) + \delta^2(L/s)}/\ln s$ .

**5. Sample Computation** In order to describe and test our numerical procedure of extracting  $d_{\text{IR}}$ , we first perform an illustrative calculation in the context of O class. In particular, we will evaluate the dimension deeply in the extended phase, namely  $d_{\text{IR}}(E=0, W=10)$  (see Table I).

To that end, we have generated ensembles for lattice sizes between  $L = 16$  and  $L = 72$ . From the set of computed lattices, seven distinct pairs  $(L/2, L)$  can be formed. We have calculated  $d_{\text{IR}}(L)$  for each of them using the relation (7) with the result shown in Fig. 1 (top) as a function of  $1/L$ . A striking feature of the obtained behavior is a clean linear approach to the infinite volume limit. However, a direct linear fit cannot be used to obtain the

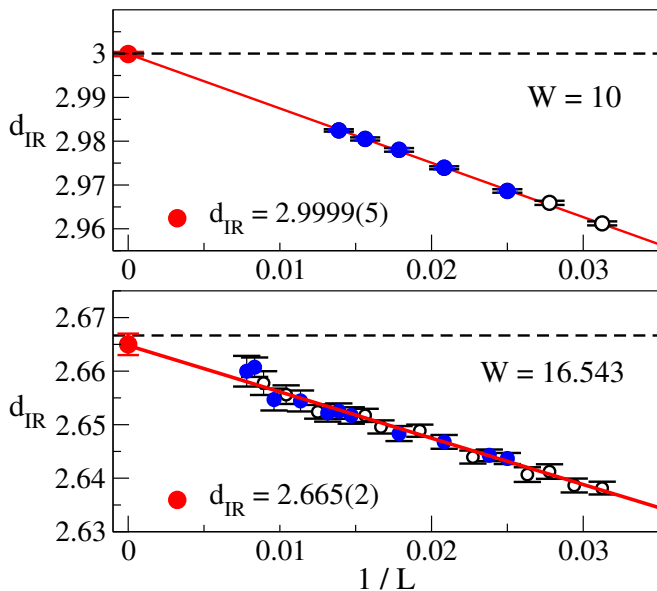


FIG. 1. Sample computation of  $d_{\text{IR}}$  for O system in the metallic regime (top) and at the critical point (bottom). Values at finite  $L$  are obtained from Eq. (7) with  $s=2$ . The horizontal dashed line in the bottom plot shows  $d_{\text{IR}}=8/3$ .

extrapolated dimension and its error. Indeed, some pairs of points in this graph are correlated since their data input involves a common lattice. One way to proceed is to select a suitable subset of mutually independent pairs to obtain a valid estimate.

In order to exactly mimic the procedure that will be used to analyze critical points, we proceed as follows. We only allow systems of sizes at least  $L_{\text{min}}=20$  to participate in the analysis and, given this cut, determine the maximal number  $K$  of independent pairs  $(L/2, L)$  that can be formed from the available data. If there is only one maximal combination, the associated linear fit determines our final estimate and its error. If there are multiple combinations, we quote the average  $d_{\text{IR}}$  over such determinations and the average error. The ensuing variability of the participating estimates characterizes the robustness of the method.

Applying the above to our  $W=10$  data (Fig. 1, top) yields  $K=5$  and a unique combination of pairs marked in blue. Note that the smallest pair is formed by lattices  $(20, 40)$  so that we are dealing with the range  $1/L \leq 0.025$ . The associated fit (shown) returns the expected value  $d_{\text{IR}}=3$  with the accuracy of couple parts in ten thousand. Note that, in this case, the resulting fit works extremely well even outside the fitting range implied by the size cut.

Following the same strategy at the critical point, we plot in Fig. 1 (bottom) the dimensions  $d_{\text{IR}}(L)$  for available pairs of sizes. We collected data for 29 lattices satisfying the size cut, producing  $K=11$  with 128 distinct combinations. One of them is visualized by blue points and the corresponding linear fit. The result is close to  $d_{\text{IR}}=8/3$  (dashed line) and error about one part per mill.

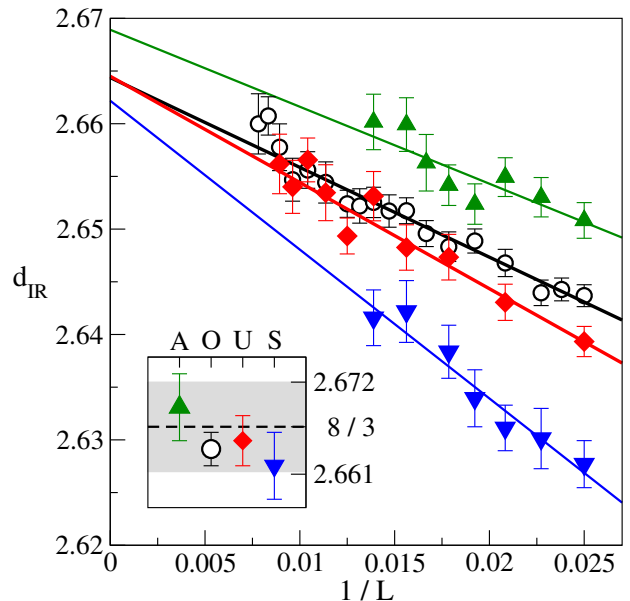


FIG. 2. Dimension  $d_{\text{IR}}$  vs  $1/L$  for  $L \geq 40$ , obtained from Eq. (7) with  $s=2$ . The inset shows infinite-volume extrapolation for each class. The shaded area marks the band with deviation less than 2 parts per mill from  $d_{\text{IR}}=8/3$ .

**6. The Results.** We will now apply the above strategy to the computation of  $d_{\text{IR}}$  at known critical points  $(0, W_c)$  of Anderson models from four universality classes shown in Table I. Empirically chosen overall size cut  $L_{\text{min}}=20$  will be imposed in the analysis since it ensures good scaling properties for all models considered.

The grand summary of all utilized data is shown in Fig. 2. The feature immediately standing out is that dimensions for O and U classes become essentially equal in the statistical sense for  $1/L \lesssim 0.02$ , approaching together the value  $d_{\text{IR}} \approx 8/3$  in the infinite-volume limit. At the same time, S and A dimensions tend to a very similar value in more disconnected manner.

The data in Fig. 2 leads to  $K_O=11$  [128],  $K_U=7$  [8],  $K_A=7$  [1] and  $K_S=7$  [1], where the subscript refers to a symmetry class and the bracket specifies the number of distinct maximal pair combinations. The corresponding final estimates of  $d_{\text{IR}}$  are given in Table I. They are also shown graphically in the inset of Fig. 2. In order to represent these final answers faithfully, the straight lines for O and U in Fig. 2 are the averages from fits over all maximal combinations. The standard deviation in the associated population of (correlated) estimates is smaller than the statistical error by about a factor of two in both cases. This confirms the robustness of the method used to obtain the extrapolated  $d_{\text{IR}}$ .

**7. The Discussion.** The properties of Anderson critical points, as expressed by the index  $\nu$ , are known to vary by as much as tens of percents (Table I). This is to be contrasted with our results for the effective spatial dimensions  $d_{\text{IR}}$  which differ at the level of couple parts per mill at most. In fact, the remaining statistical and

mild systematic (entering via  $L_{\min}$ ) uncertainties open the possibility that  $d_{\text{IR}}$  may be strictly *super-universal*, taking the value of approximately 8/3 at Anderson transitions.

The relevance of critical  $d_{\text{IR}}$  is that it describes the geometry of *physical* space involved in an Anderson transition in the same way as Minkowski or Hausdorff dimensions describe the geometry of fractal sets. Its meaning can be illustrated by a fictional inquiry about the properties of space, addressed to Anderson electrons ( $E=0$  eigenstates). The response from O-electrons may read like this: “While our probing means are limited, this is what we can say. If space is sprinkled with disorder of strength  $W < W_c$ , then doubling the lengths in all directions gives us  $2^3$  times more volume to effectively spread into when these lengths are large. Hence, we see space as 3-dimensional. But when disorder of strength  $W > W_c$  is used, this factor converges to unity ( $2^0$ ) for large lengths, and the space acts 0-dimensional. Most interestingly, when  $W = W_c$ , our effective volume grows by the factor close to  $2^{8/3}$  and we have no choice but to tell you that the dimension of space we experience in this case is about 8/3.”

Super-universality of  $d_{\text{IR}}$  conveys that the response from U, S, and A-electrons, and possibly others, will be identical to the one above. In other words, that the most basic characteristic of spatial geometry involved in an Anderson transition – the dimension through which it proceeds – is insensitive to the symmetries involved. Rather, it is entirely determined by the defining attribute of these transitions as changes from diffusive to non-diffusive dynamical regimes of quantum particles subject to spatial disorder. The proposed super-universal status could make  $d_{\text{IR}}$  a fingerprint of the Anderson phenomenon.

Our reasoning is made possible by the effective number theory [9, 10] which gives the effective volume based on Eq. (1) its measure-like character and reveals its absolute meaning. Conversely, the growing evidence that the associated  $d_{\text{IR}}$  leads to productive results (see also [11]) confirms the usefulness of the underlying ideas. The conceptual basis of  $d_{\text{IR}}$  is in fact even more solid due to the *effective dimension theory* which formalizes the notion of measure-based dimension for probability-induced effective subsets [12]. Within this framework, it can be shown that there only exists one dimension which coincides with  $d_{\text{IR}}$ .

One may inquire about a more precise meaning of critical  $d_{\text{IR}}$  in light of the commonly discussed structure of dimensions in the critical state (see e.g. [17–19] or reviews [4, 20]). Although the dimensions invoked in such considerations are different from the one studied here, we do expect the critical state to be dimensionally non-trivial in the usual geometric sense. Since  $d_{\text{IR}}$  reflects ordinary geometry, it produces the largest dimension present in a composite object, similarly to standard dimensions such as Hausdorff, Minkowski or topological. Related issues will be elaborated upon elsewhere.

Among motivations leading to  $d_{\text{IR}}$  was a need for such characteristic in studies of Dirac modes in Quantum Chro-

modynamics (QCD). One recent novelty in that area is a power singularity of mode density at eigenvalue  $\lambda_{\text{IR}}=0$ , appearing in thermal QCD at certain temperature. Its existence sparked the proposal for a new scale-invariant phase of strongly interacting matter [21]. The vicinity of  $\lambda_{\text{IR}}$  was shown to have certain properties normally associated with localization [11, 22], suggesting that it can be viewed as a critical point of Anderson type. In addition, there is a known Anderson-like point  $\lambda_A$  in the bulk of the spectrum [23–25]. These developments raise interesting questions about the degree of similarity between such QCD features, arising from rather complicated dynamics, and pure Anderson transitions. The results presented here and further studies of  $d_{\text{IR}}$  in both contexts will likely help to resolve such questions.

P.M. was supported by Slovak Grant Agency VEGA, Project n. 1/0101/20. I.H. acknowledges the discussions with Andrei Alexandru and Robert Mendris.

---

\* [ihorv2@g.uky.edu](mailto:ihorv2@g.uky.edu)

† [peter.markos@fmph.uniba.sk](mailto:peter.markos@fmph.uniba.sk)

- [1] P. W. Anderson, *Phys. Rev.* **109**, 1492 (1958).
- [2] E. Abrahams, P. W. Anderson, D. C. Licciardello, and T. V. Ramakrishnan, *Phys. Rev. Lett.* **42**, 673 (1979).
- [3] E. Abrahams, *50 Years of Anderson Localization*, International journal of modern physics: Condensed matter physics, statistical physics, applied physics (World Scientific, 2010).
- [4] F. Evers and A. D. Mirlin, *Reviews of Modern Physics* **80**, 1355 (2008).
- [5] F. J. Wegner, *Zeitschrift für Physik B* **25**, 327 (1976).
- [6] A. MacKinnon and B. Kramer, *Phys. Rev. Lett.* **47**, 1546 (1981).
- [7] K. Slevin and T. Ohtsuki, *Phys. Rev. Lett.* **82**, 382 (1999).
- [8] K. Slevin and T. Ohtsuki, *Journal of the Physical Society of Japan* **87**, 094703 (2018).
- [9] I. Horváth and R. Mendris, *Entropy* **22**, 1273 (2020), [arXiv:1807.03995](https://arxiv.org/abs/1807.03995) [quant-ph].
- [10] I. Horváth, *Quantum Rep.* **3**, 534 (2021), [arXiv:1809.07249](https://arxiv.org/abs/1809.07249) [quant-ph].
- [11] A. Alexandru and I. Horváth, *Phys. Rev. Lett.* **127**, 052303 (2021), [arXiv:2103.05607](https://arxiv.org/abs/2103.05607) [hep-lat].
- [12] I. Horváth and R. Mendris, in preparation.
- [13] Y. Asada, K. Slevin, and T. Ohtsuki, *Journal of the Physical Society of Japan* **74**, 238 (2005).
- [14] T. Wang, T. Ohtsuki, and R. Shindou, *Physical Review B* **104** (2021), [10.1103/physrevb.104.014206](https://doi.org/10.1103/physrevb.104.014206).
- [15] K. Slevin and T. Ohtsuki, *Phys. Rev. Lett.* **78**, 4083 (1997).
- [16] M. Bollhöfer and Y. Notay, *Comp. Phys. Comm.* **177**, 951 (2007).
- [17] A. Mildenberger, F. Evers, and A. D. Mirlin, *Physical Review B* **66** (2002), [10.1103/physrevb.66.033109](https://doi.org/10.1103/physrevb.66.033109).
- [18] L. J. Vazquez, A. Rodriguez, and R. A. Römer, *Physical Review B* **78** (2008), [10.1103/physrevb.78.195106](https://doi.org/10.1103/physrevb.78.195106).
- [19] A. Rodriguez, L. J. Vazquez, and R. A. Römer, *Physical Review B* **78** (2008), [10.1103/physrevb.78.195107](https://doi.org/10.1103/physrevb.78.195107).

- [20] P. Markoš, *Acta Physica Slovaca. Reviews and Tutorials* **56** (2006), 10.2478/v10155-010-0081-0.
- [21] A. Alexandru and I. Horváth, *Phys. Rev. D* **100**, 094507 (2019), [arXiv:1906.08047 \[hep-lat\]](#).
- [22] A. Alexandru and I. Horváth, (2021), [arXiv:2110.04833 \[hep-lat\]](#).
- [23] T. G. Kovacs and F. Pittler, *Phys. Rev. Lett.* **105**, 192001 (2010), [arXiv:1006.1205 \[hep-lat\]](#).
- [24] M. Giordano, T. G. Kovacs, and F. Pittler, *Phys. Rev. Lett.* **112**, 102002 (2014), [arXiv:1312.1179 \[hep-lat\]](#).
- [25] L. Ujfalusi, M. Giordano, F. Pittler, T. G. Kovács, and I. Varga, *Phys. Rev. D* **92**, 094513 (2015), [arXiv:1507.02162 \[cond-mat.dis-nn\]](#).